2011 NDIA GROUND VEHICLE SYSTEMS ENGINEERING AND TECHNOLOGY SYMPOSIUM
MODELING & SIMULATION, TESTING AND VALIDATION (MSTV) MINI-SYMPOSIUM
AUGUST 9-11 DEARBORN, MICHIGAN

A Multi-Dimensional Battery Discharge Model with Thermal Feedback Applied to a Lithium-ion Battery Pack

Donald E Neumann, Ph.D
Senior Engineering Specialist
Electrical Power & Energy
General Dynamics Land Systems
Sterling Heights, MI

Scott Lichte
Technical Product Manager
EnerSys Energy Products
Warrensburg, MO

ABSTRACT

With the growing complexity of electrical and electronic subsystems on modern vehicle platforms, performance of the battery becomes an ever-increasing concern for the user and consequently a key technical focus for the developer. Detailed models are germane for accurate predictions and assured performance. Models should include parameters and variables for the multitude of conditions that affect the output. Whereas many traditional models only account for coulombic discharge capacities (i.e. amp-hours) a complete model must predict terminal voltage to provide for an accurate energy estimator. This aspect is most important as real-world performance is impacted by the mix of resistive and constant-power loads on the vehicle. In particular, constant-power loads will draw increasing amounts of current and/or run longer when the voltage is reduced. Using battery manufacturer data, a multi-dimensional model is provided. The model accounts for the previously mentioned variables as well as the internal thermal heating of the battery during discharge conditions.

INTRODUCTION

Battery discharge models play an ever-increasing role in today's products, owing to greater numbers of battery-dependent products and increasing customer expectations for reliable prediction of the equipment status and battery condition. Vehicular system designs share this expanding need along with consumer electronic products. In the past, this need was focused primarily in two areas: vehicle starting, and silent watch capability (for military vehicles used in operations that require silent watch). More recently, emerging vehicle designs have included additional electronic subsystems and components with built-in "hold-up" batteries as well as batteries for dismounted operations. Hybrid- and electric-drive vehicles will place further demands for reliable models and their prediction capabilities.

Traditionally, the battery model has played a key role in the vehicle design phase in order to fully specify and assess the energy storage subsystem (ESS). Today, battery models have become an important technology for the development of battery monitor subsystems. Expanded roles for the ESS models span the vehicle's operational lifetime, including use for logistics predictions, prognostics, mission planning and vehicle capability assessments.

DEFINITIONS

The fundamental battery condition parameters include state-of-health and state-of-charge. The state of charge (SOC) is the amount of charge available compared to the present capacity of the battery to hold charge. Perhaps more formally defined by the IEEE(Institute of Electrical and Electronic Engineers, 2000) as: "state-of-charge factor = Actual capacity of a battery expressed as a percentage of a fully-charged capacity. Note: This is based on experience, application (cycling /float service), and charging parameters." For a battery in good health, the SOC is the key measure of how much work the battery can perform.

This work may be at any discharge rate from the lowest (typically a reserve capacity) to the highest (typically a cranking rate).

The state of health (SOH) is largely a measure of the remaining functional lifetime of a battery. SOH is typically expressed as a percentage and is determined by the amount of charge the battery is able to hold compared to the normal specified new battery capacity.

When used together, the SOC and SOH fully define the ability of the battery (in any state of health) to perform work. That is:

$$Capacity_{Remain} = Capacity_{Spec} \cdot SOC \cdot SOH$$

BACKGROUND

Over the course of battery technology evolution, battery discharge models have grown from simplistic single-variable linear models to complex multi-variate non-linear models. Initially, models were limited to the battery capacity using the fundamental discharge variable defined in amp-hours.

$$Capacity_{Remain} = Capacity_{Initial} - \sum_{i} \left| Amps_i \cdot Time_i \right|$$

As engineers and scientists gained greater insight of battery technology and more data became available for specific battery types, detailed models could be developed. Typical battery curves, from measured performance, would provide users greater insight.

For military vehicles, the conditions surrounding silent watch and engine restart drove the need for information regarding battery capability. Potential mission scenarios under a wide variety of environmental and operational conditions demanded a full understanding of the batteries. The engineering community produced empirical data and associated models, typically in the form of data tables and curves. Variables included discharge rate and temperature. Several of the examples here include (Kaufmann, 1952), Karchon, and (US Army Material Command, 1974). The latter, (US Army Material Command, 1974) as a design guide utilized an empirical model with parameters from the data curves.

$$Cap_{Remain} = Cap_{Init} \cdot \left(1 - \sum_{i} \frac{CapReqd_i}{N \cdot CapAvail_i} \right)$$

With the space race in the 1960's, NASA strove to develop more detailed models for batteries and other energy sources used in spacecraft. In the late 60's, NASA began a Battery Workshop to provide government & industry focus in an area that is critical to their charter.

More recently, several battery modeling innovations have transcended the engineering community. In 2002 (Gao, Liu, & Dougal, 2002) introduce a dynamic model, suitable for virtual prototype applications which they apply to the commercial 18650 lithium-ion battery. This model includes both state of charge and ambient temperature within empirical formulae in their model. In (Chen & Rincon-Mora, 2006) nonlinear open-circuit voltage is included along with storage time-dependent capacity and transient response characteristics. A variety of extended response characteristics are discussed to account for current, temperature, and cycle number dependencies. Another, (Tremblay, Dessaint, & Dekkiche, 2007), provides a superior means of simulating a complete discharge profile, starting with the open circuit terminal voltage and including an initial exponential transient, a nominal discharge profile region and the sharp voltage roll-off as the battery is exhausted.

APPLICATION

As with many prior model developments, new battery types combined with vehicle applications present a need for greater understanding of the battery's capabilities. In this particular case, various battery packs were being considered for use as a silent watch energy source for a potential vehicle upgrade project. Among several candidates, the EnerSys MPS-series provided modular units in a package size that fit well in an available vehicle space claim, see Figure 1 - EnerSys MPS300 battery pack. The MPS was a new product line … the MPS300 and MPS350 were specifically designed for defense applications. The units are environmentally sealed and have innovative electronic features that allow them to be directly compatible with a MIL-STD-1275 power bus even when operating in parallel with lead-acid batteries.

Figure 1 - EnerSys MPS300 battery pack

Available data on actual MPS300 performance (Figure 2 - Battery discharge curve data) demonstrated many of the known and expected attributes of lithium-ion batteries. The consistent discharge capacity, good energy density, no memory effect, and minimal loss of capacity when not in use were favorable. Another known attribute was a modest initial voltage droop during severe cold operation; see the 60 amp discharge curve at -46°C (dark solid blue line shown in Figure 2). This condition is characteristic of electro-chemical cells as chemical activity increases with higher temperature and decreases as temperature decreases. In the case of cells with liquid electrolyte, as the electrolyte approaches the freezing point, the performance of the battery falls off dramatically. In the case of lithium-ion batteries, however, an initial discharge pulse can generate sufficient heat to unthaw the electrolyte and provide suitable performance thereafter.

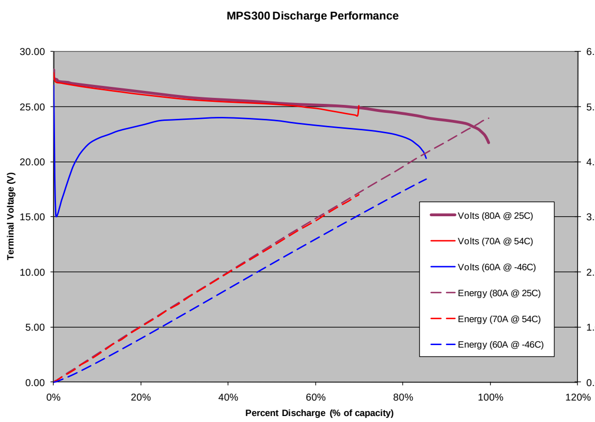

Figure 2 - Battery discharge curve data for EnerSys MPS300V28C184SC

A more complete battery model is needed to account for the visible droop and the overall performance at lower temperatures.

MODEL FORMULATION

The necessary battery model would require a basic model with temperature-dependent parameters as well as thermal feedback and internal heating response characteristics. The basic model would account for internal resistance as well as a long-term transient and discharge roll-off. These basic characteristics had been included, to some extent, in models by Chen & Rincon-Mora, Gao, and Tremblay. Temperature dependency is added to the basic model so that the internal heating can affect the electrical output.

The addition of thermal feedback provided a means to correctly depict the characteristic initial voltage droop recovery during extreme cold discharge. The heat generated from the initial current surge through the internal resistive elements results in warming of the battery materials. The heat coefficients, thermal mass, and heat dissipation (to the external ambient) results in a differential equation for the solution space. The feedback (internal temperature rise) directly influences the series resistive elements to provide recovery from the voltage droop and favorable conditions for continued battery use. Hence, the combined aspects of temperature-dependency together with thermal feedback provide this particular model with unique response characteristics.

The basic model is depicted in Figure 3 - Fundamental electrical portion of battery model. To simplify the initial solution, the short-term transient & AC characteristics were not included. These characteristics are typically represented by an RC circuit; as in Figure 3, they are R1 and C1. However, the energy content from these elements is negligible when compared to the overall discharge energy. The goal is to predict the available discharge energy, wherein the short (~ 1 second or less) burst that these elements represent would not be a contributor and only complicate the initial parameter solution.

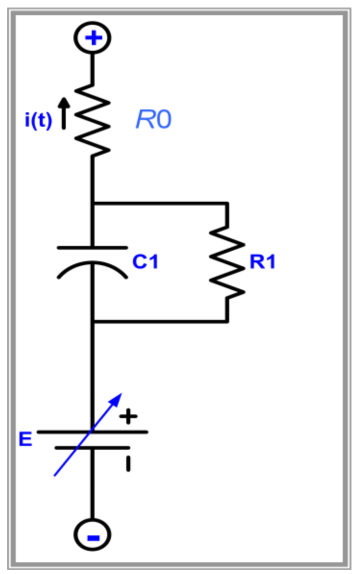

Figure 3 - Fundamental electrical portion of battery model

The thermal feedback for the complete model is shown in Figure 4 - Complete battery model used for initial solutions. The differential equation for the internal temperature is as follows.

$$\mathrm{Tint}(t) = \frac{1}{\mathrm{Cth}} \cdot \int_{t_0}^{t} \mathrm{Qth}(\tau)\, d\tau - \frac{1}{\mathrm{Rth}\cdot\mathrm{Cth}} \cdot \int_{t_0}^{t} \left(\mathrm{Tint}(\tau) - \mathrm{Ta}\right) d\tau + \mathrm{Tint}(t_0)$$

The variables used in the overall model are described in Table 1 Table of variables. Note that this set of equations does not explicitly include heat of reaction. However, the subsequent solution for the thermal feedback parameters account for this heat. The solution is based on actual data so that the reaction heat ends up in the resulting empirical model even though there are no parameters or variables for the heat of reaction.

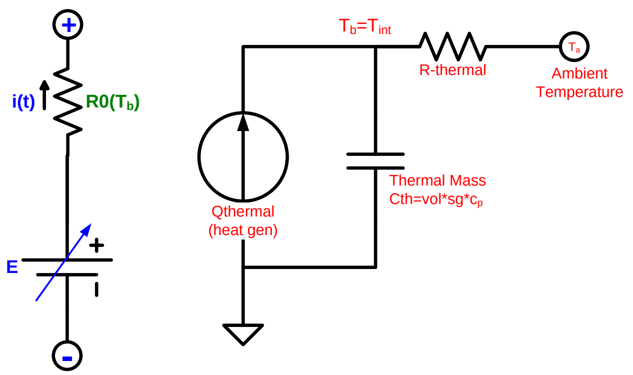

Figure 4 - Complete battery model used for initial solutions

The complete system of equations is shown in Figure 5. The equation in green background defines the internal resistance using an exponential function of temperature with an offset parameter (gamma). The pair of equations in the blue background define the internal voltage source (E) as a function of the cumulative discharge, . The internal voltage will also be the open-circuit terminal voltage. The set of equations shown with the orange background define the relationships among the heat generated, ambient temperature, internal heat gain, external heat loss, and the resulting impact on the internal temperature. As depicted, these three sets of equations feed the overall definition of the terminal voltage (i.e. shown with grey background) for any time (t) and temperature (T).

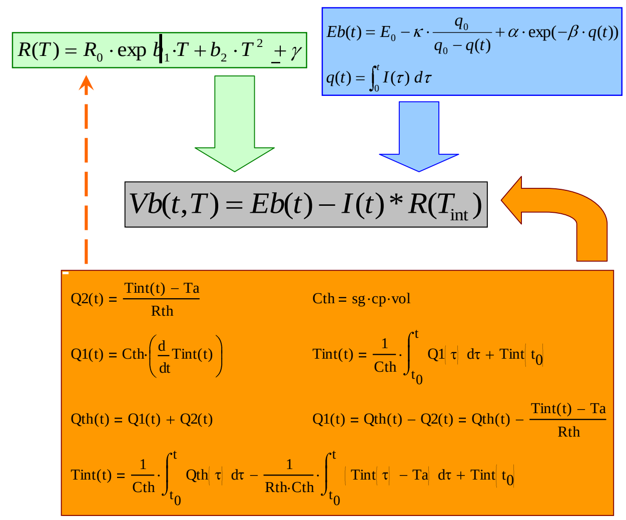

Figure 5 - System of equations for model

Table 1 Table of variables

Name	Quantity	Units
Tint	Internal temperature	°K
Cth	Thermal mass	(W-sec)/Δ°K
Qth	Generated heat	watt
Rth	Thermal resistance	Δ°K/W
Ta	Ambient temperature	°K
R0	Series resistance	Ohm
E	Internal voltage	Volt
t	Time	sec
t_0	Initial time	sec

PARAMETER DEFINITIONS

The key parameters for this model were determined using specification data and measured discharge curves provided by EnerSys. A partial family of curves is shown in Figure 2. A portion of the specification sheet is included as an appendix. Initial estimates were used as seed values for numerical convergence in recursive multivariate solutions. Explicit least-mean-square error solutions were used for most of the basic parameters for the discharge model. Collectively, the result is provided here in Table 2 - Table of battery model parameters. The background colors in this table correspond to their use within Figure 5 - System of equations for model.

Table 2 - Table of battery model parameters

Ro	66683941249	(ohm)
b1	-0.184	(-)
b2	0.000297834	(-)
gamma	-22	(m-ohm)
To	273.15	(K)
Eo	25.6	(volt)
kappa	0.220786	(volt)
q0	170	(A-hr)
alpha	2.813797	(volt)
beta	0.017845789	1/(A-hr)
delta	0	(volt)
sg	1.47132243	(g/mL)
cp	0.2	(cal/(g-°C))
Rth	2	(°C/W)
Cth	46808.424	(W-s/°C)

ASSESSMENT

Using the parameters from Table 2, 3-dimensional curve data sets were developed for 15, 20, and 60 amp discharge conditions over a temperature range of -46°C to +41°C. Contour graphics for each of these discharge rates are shown in Figure 6, Figure 7, and Figure 8. The curve surfaces depict the terminal voltage as the battery discharges to 5% remaining capacity. Note that the voltage droop at the coldest temperature becomes more observable at the higher discharge rate (60A). That is, the model exhibited characteristics very similar to those seen in the battery data.

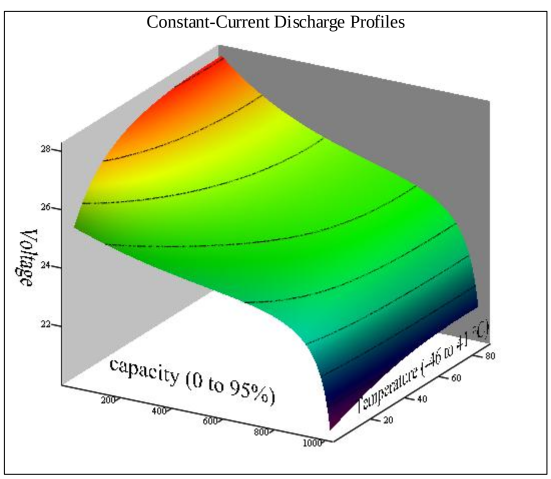

Figure 6 - Discharge voltage: 15 amp; -46°C to +41°C; from full capacity

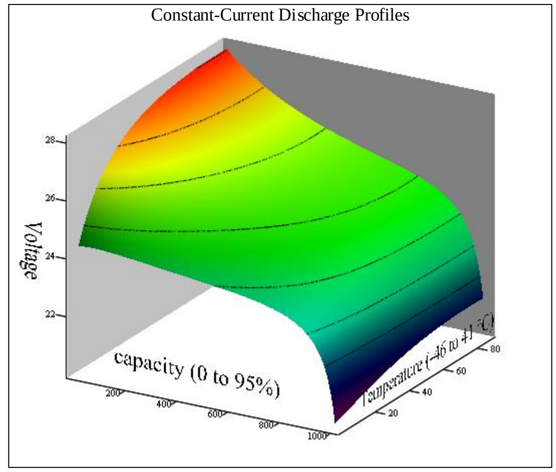

Figure 7 - Discharge voltage: 20 amp; -46°C to +41°C; from full capacity

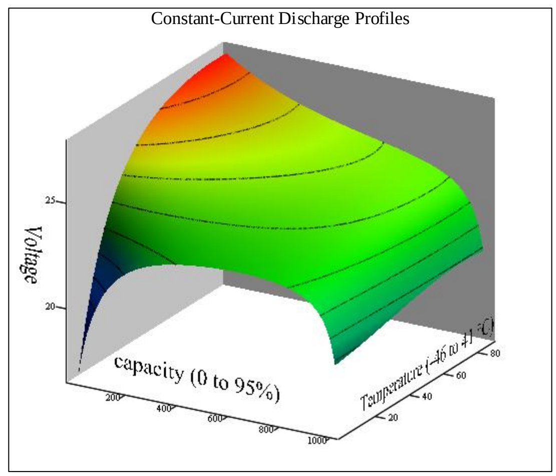

Figure 8 - Discharge voltage: 60 amp; -46°C to +41°C; from full capacity

To better assess the accuracy of the results, a slice of data was extracted, corresponding to the temperature condition in the original (2-dimensional) data curves. This "slice" was then compared to the original data. The curve comparison for the 60 amp discharge condition is shown in Figure 9 – Comparison of 60A discharge responses: model prediction vs. original battery data. In this figure, the model prediction is in red (solid curve labeled X60) and the original battery discharge test data is in blue (dashed curve, labeled vt60). As seen in comparing the two 60 amp discharge curves for -46°C, the overall response is very realistic. A closer comparison reveals that the real-world thermal response appears to be faster than what is predicted by the current model.

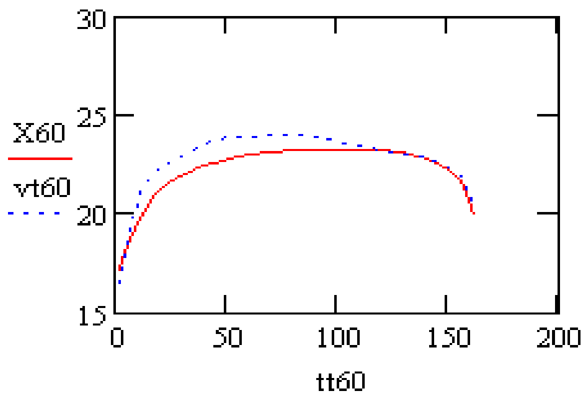

Figure 9 – Comparison of 60A discharge responses: model prediction vs. original battery data

Aggregate results are compared in Table 3 – Comparison of model and original data; 60 amp discharge at -46°C. The discharge time, initial droop voltage, and total discharge energy are shown to be reasonably close. From this table, estimates for the model errors are -0.3% for discharge time, +6.5% for minimum droop voltage, and -2% for total energy. As noted, calculations using a flat terminal voltage assumption would (incorrectly) predict a higher energy output, which would be off by more than 10%.

Table 3 – Comparison of model and original data; 60 amp discharge at -46°C

60A @ -46°C	Model	Data
Discharge Time	161.5 min	162 min
Initial Droop	16.2 volt	15.2 volt
Energy	12.96 MJ	13.25 MJ

NOTE: 160 A-hr @ 25.6 V = 14.75 MJ

CONCLUSIONS & RECOMMENDATIONS

Overall, the response surfaces would appear to be very realistic. The combined aspects of temperature-dependency together with thermal feedback provide this particular model with unique response characteristics. In particular, the characteristics at extreme cold conditions provide an accurate depiction of the measured response. Hence, the modeling approach is deemed valid.

However, as the real-world thermal response is faster than what is predicted by the model, further model parameter tuning is warranted. The results from additional battery testing & data will help to further refine this model.

Application of this modeling approach for other battery products is recommended.

REFERENCES

Bibliography

Chen, M., & Rincon-Mora, G. (2006). Accurate Electrical Battery Model Capable of Predicting Runtime and I–V Performance. *Transactions on Energy Conversion, IEEE* , 504-511.

Gao, L., Liu, S., & Dougal, R. (2002). Dynamic Lithium-Ion Battery Model for System Simulation. *IEEE Transactions on Components and Packaging Technologies* , 495-505.

Institute of Electrical and Electronic Engineers. (2000). *The Authoritative Dictionary of Standard Terms, IEEE Standard 100.* New York, NY: IEEE Press.

Kaufmann, R. &. (1952). *DC Power Systems for Aircraft.* John Wiley & Sons.

Tremblay, O., Dessaint, L., & Dekkiche, A.-I. (2007). A Generic Battery Model for the Dynamic Simulation of Hybrid Electric Vehicles. *IEEE Proceeding of the Vehicle Power and Propulsion Conference, VPPC 2007* , 284-289.

US Army Material Command. (1974). *Engineering Design Handbook - Military Vehicle Electrical Systems.* Warren: US AMC.

Acknowledgement

This work was supported by Stryker Modernization project SPGCBLD207, funded in part by the Stryker Program under contract SHC-L112, Delivery Order 0121.

APPENDIX A

MPS300 SERIES SPECIFICATIONS	
Charge Voltage	28.2± 0.3V
Nominal Voltage	25.6V
Cut-off Voltage	21.0V
Cycle Life @ 80% DOD	1800
Cycle Life @ 50% DOD	8000
Peak Charge/Discharge Current (5sec)	100A
Max. Charge/Discharge Current (25°C)	75A
Max. Charge/Discharge Current (60°C)	50A
Terminals	M8-1.25 female threaded
Operating Temperature	-40 to 131°F (-40 to +55°C)
Storage Temperature	-67 to 149°F (-55 to +65°C)